Spectrophotometry

Temperature-dependent enzyme kinetics monitored through UV-Visible absorption measurements

Introduction

Enzymes are macromolecules which act as catalysts in a variety of biological reactions. As a catalyst, an enzyme aids in increasing the rate of the reaction by lowering the activation barrier for the reaction (Figure 1), providing a more energetically favorable reaction pathway. These reactions involve the interaction of a substrate with the active site on an enzyme, which in turn leads to the formation of a given product. A variety of application spaces, like pharmaceutical or food manufacturers, will often conduct studies to assess these types of reactions. In these circumstances, researchers are interrogating whether their products are able to either impede or facilitate a specific enzymatic pathway.[1,2] As such, it is important to be able to monitor these reactions under a variety of experimental conditions in order to better understand the dynamics. This information directly aids in establishing the optimum reaction conditions.

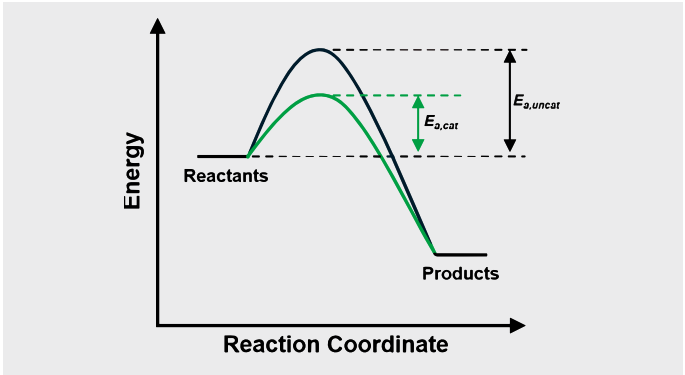

Figure 1: Reaction profile for reactions with (green) and without (black) a catalyst. The double-sided arrows represent the activation energy need to overcome the energy barrier with ($E_{a,cat}$) and without ($E_{a,uncat}$) a catalyst.

Enzymatic reactions are highly dependent on the substrate concentration. In such reactions, increasing the substrate concentration leads to an increased reaction rate. However, as these biological reactions involve complexation of the substrates to the active sites on the enzyme, the number of available active sites acts as a limiting reagent for the reaction. Once the active sites are fully saturated, increasing the substrate concentration no longer results in improvements to the reaction rate. This behavior can be modeled by the Michaelis-Menten equation (Eqn. 1),

$$v = \frac{V_{\max}[S]}{K_m + [S]} \quad (1)$$

where v is the calculated reaction rate as a function of substrate concentration; V_{max} is the maximum reaction rate; $[S]$ is the substrate concentration; and K_m is the Michaelis constant, the substrate concentration at which half of the active sites on the enzyme are occupied.[3] In practice, the enzymatic reactions are performed multiple times using different substrate concentrations and plotted as a function of $[S]$. Through fitting the data to the Michaelis-Menten function, V_{max} and K_m can be determined. As these parameters are helpful in assessing the optimal conditions for an enzymatic reaction, this analysis is often carried out in research environments. More details pertaining to the Michaelis-Menten kinetic analysis are included elsewhere.[4]

Like many other non-biological reactions, temperature can play an important role in the overall dynamics of a reaction. An increase in temperature leads to the transfer of kinetic energy to the molecules in solution, causing faster collision rates, and therefore faster reaction times. However, the stability of the enzyme must also be accounted for as with higher temperatures the enzyme can denature, leading to a loss of the catalyst. This loss will lead to a greatly diminished reaction rate, as shown in Figure 2.[5] The temperature which leads to the highest reaction rate without significant enzyme degradation is considered optimal.

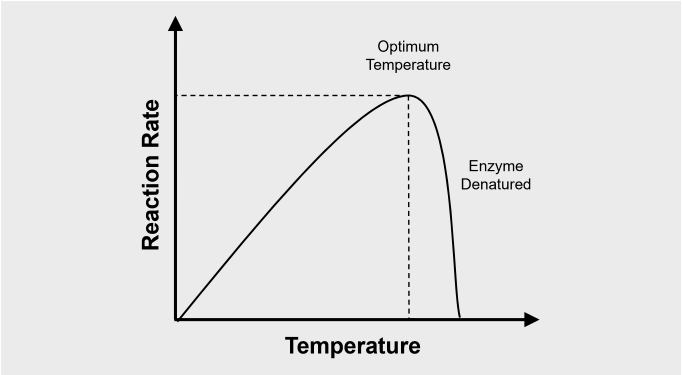

Figure 2: Generic demonstration of how an enzymatic reaction rate is influenced by temperature.

In many reactions, one or more of the reactants and products can be analyzed using UV-Visible absorption spectroscopy. This technique uses light in the UV-Visible spectral range to interrogate electronic transitions in molecules. When photons with energy greater than or equal to the energy difference between the electronic ground and excited states interacts with an analyte, it induces these transitions. UV-Visible instruments detect the loss of light intensity at specified wavelengths in the UV-Visible range when the photon is absorbed, and can report this intensity loss in terms of absorbance units. By its nature this technique is non-destructive, allowing for further analysis of the sample by other means after the UV-Visible measurement is completed.

According to Beer's law (Eqn. 2),

$$A_\lambda = cle_\lambda \quad (2)$$

where A_λ is the measured absorbance at the specified wavelength (λ), l is the path length, ε_λ is the molar absorptivity and c is the analyte concentration, the absorbance of a material is directly proportional to the concentration of the analyte. Due to the correlation between absorbance and concentration, UV-Visible absorption measurements are often conducted to monitor the loss or gain of an absorptive compound as a function time. This data can then be used in kinetic analysis to assess the reaction rates. For enzymatic reactions, these reactions rates are needed to perform a Michaelis-Menten kinetic analysis, as outlined previously.

Due to the nature of this analysis, multiple samples with varying reactant concentrations must be monitored over the course of the reaction. Without the use of a multi-cell changer, each reaction needs to be monitored individually, leading to a longer overall experiment time. This is especially cumbersome for temperature-dependent measurements where the same set of reactions need to be repeated at various temperatures. By using a temperature-controlled multi-cell changer, these reactions can be performed simultaneously, leading to a substantial improvement in the time needed to complete the measurements. This can be particularly useful if the samples studied are easily degraded over time.

Herein, the reaction between guaiacol and hydrogen peroxide (H_2O_2) catalyzed by horseradish peroxidase (HRP),[6,7] shown in Figure 3, is used to demonstrate the temperature-dependent reaction kinetics of enzymatic systems. The reactions were monitored through UV-Visible absorption measurements carried out using the Thermo Scientific™ Evolution™ One UV-Visible Spectrophotometer equipped with a Thermo Scientific™ 6-cell Rotary Peltier. The experiments included demonstrate the degree at which temperature can influence the overall kinetic profile of an enzymatic reaction. As described, this information can be critical to understanding the optimal conditions at which an enzymatic reaction should be performed.

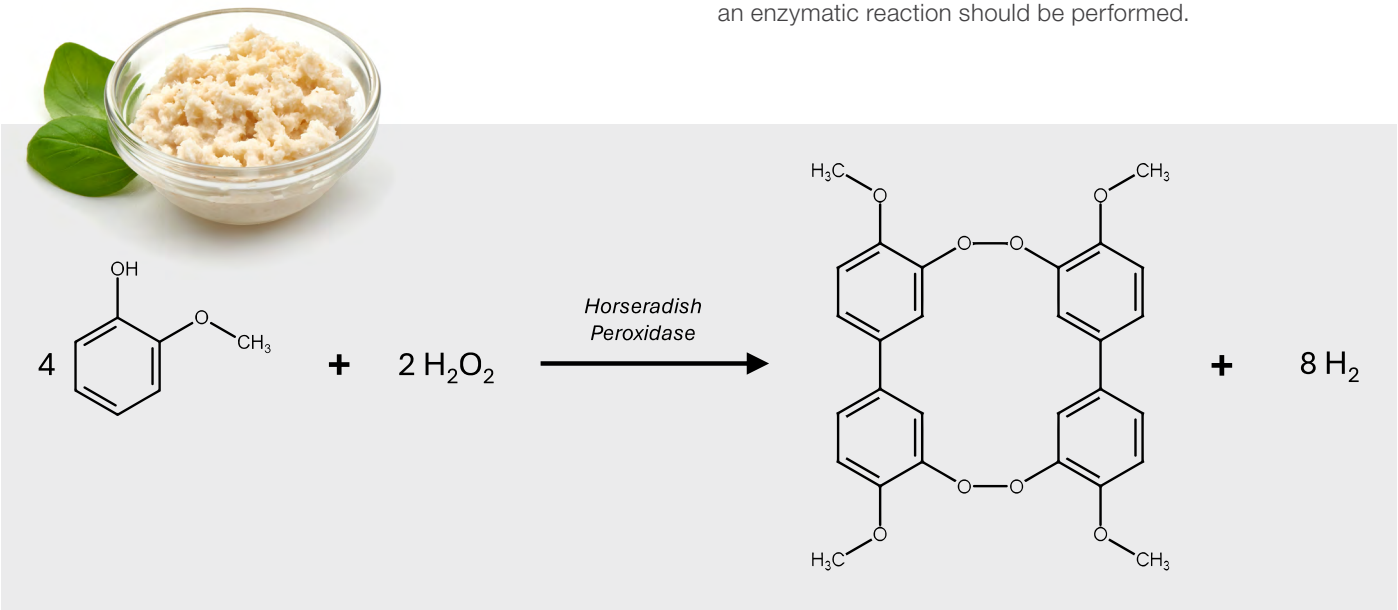

Figure 3: Reaction between guaiacol and H_2O_2 catalyzed by horseradish peroxidase.

Experimental

Samples preparation

Samples were prepared and subsequently analyzed based on the experimental procedure outlined in Shannon et. al.[6] Briefly, a 3838 nM stock solution of HRP was prepared by dissolving 7.6 mg of HRP in 45 mL of phosphate buffer (1X PBS). A subsequent dilute HRP stock solution was then made by diluting 130 µL of the 3838 nM stock HRP solution with 9.87 mL of PBS, yielding a concentration of 50 nM HRP. A 45 mM solution of guaiacol was prepared by diluting 374 µL of guaiacol (99%, used as received) to a total volume of 75 mL with DI water. A 1.0 M stock solution of H_2O_2 was prepared by diluting 391 µL of 30% H_2O_2 with 4.609 mL DI water. 150 µL of the 1 M H_2O_2 stock solution was diluted to a total volume of 10 mL using DI water to prepare the 15 mM H_2O_2 stock solution. Five separate reaction samples were prepared as described in Table 1. These samples were remade fresh for each of the five reaction temperatures used.

Sample number	Volume 50 nM HRP (µL)	Volume 45 mM Guaiacol (mL)	Volume 15 mM H_2O_2 (µL)	Volume 1X PBS (mL)
1	53.0	1.00	10.0	1.937
2			20.0	1.927
3			40.0	1.907
4			60.0	1.887
5			80.0	1.867

Table 1: Sample preparation for kinetics experiments.

Instrument parameters

Absorbance measurements as a function of time were acquired using an Evolution One Spectrophotometer equipped with the 6-cell rotary Peltier cuvette holder. The absorbance at 470 nm was monitored every 15 s for 180 s. A 1.0 s integration time and 1.0 s dwell time were used. The spectral bandwidth was set to 1.0 nm and each sample was held in a 1.0 cm quartz cuvette. A stir bar spun at 400 rpm was used to ensure the solutions were heated evenly throughout the course of the experiment.

Individual blank measurements were collected in each sample position through the "Multi-Zero" function within the Thermo Scientific™ Insight™ Pro Software. The blank solutions were prepared like the sample solutions were prepared (Table 1) except the 50 nM HRP was not added. After the blanks were collected, and without removing the cuvettes, the reaction was initiated with the addition of the 50 nM HRP stock solution as outlined in Table 1 and the measurements were begun.

The experiment was performed a total of five separate times. Each time, the 6-cell rotary Peltier cuvette holder and associated temperature controller was used to maintain the solution temperature over the course of the experiment. The maintained temperatures for each experiment set were 25 ˚C, 35 ˚C, 45 ˚C, 55 ˚C and 65 ˚C.

Results and discussion

Figure 4a includes the resulting kinetic traces for the reaction between guaiacol and H_2O_2 catalyzed HRP, as described previously. These reaction kinetics were measured while each solution was held at 35 ˚C. The change in absorbance over time fits well to a linear function for each H_2O_2 concentration, implying the reaction adheres well to a zeroth order reaction profile. This behavior is expected as the enzyme act as a catalyst in this reaction, in which the reactants need to interact with the enzyme surface to initiate the reaction. Like other catalytic reactions, this will typically manifest as a zeroth order reaction. Table 2 includes the calculated rate constants for the reaction at 35 ˚C. The rate constant was calculated within the Insight Pro Software and converted to µM/s units from A.U./s units through Beer's law using the molar absorptivity at 470 nm for tetraguaiacol (26600 M^{-1} cm^{-1}).[7]

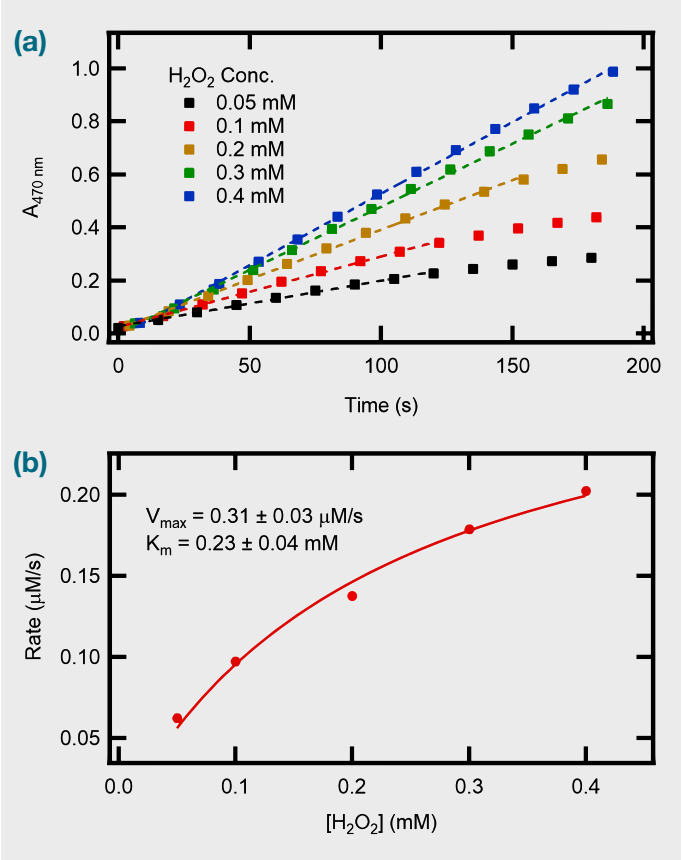

Figure 4: (a) Kinetic traces of tetraguaiacol formation in the presence of 0.877 nM HRP and 15.8 mM guaiacol. Included are traces monitored at 470 nm with varying H_2O_2 concentrations all held at 35 ˚C. Dashed lines indicate linear fits to the kinetic profile. (b) Michaelis-Menten plot for data collected at 35 ˚C.

As is shown in Table 2, increasing the concentration of H_2O_2 leads to a faster reaction rate, denoted by a larger rate constant. With more H_2O_2 molecules present in solution, the probability of collisions between reactants increases, leading to a higher reaction rate. Figure 4b includes the Michaelis-Menten plot for the reactions depicted in Figure 4a. From the fitting parameters, V_{max} and K_m were found to be 0.31 ±0.03 µM/s and 0.23 ± 0.04 mM, respectively.

H_2O_2 concentration (mM)	Zeroth order rate constant (µM/s)
0.05	0.0624
0.1	0.0974
0.2	0.138
0.3	0.179
0.4	0.203

Table 2: Calculated rate constants for the HRP-catalyzed formation of tetraguaiacol held at 35 ˚C.

As described previously, temperature can have a significant impact on the reaction rate. Consequently, it can be important to determine the optimal temperature at which the reaction can be carried out. This temperature may be used to ensure the reaction happens as quickly as possible to out-compete side reactions. Additionally, the optimal temperature is often the temperature at which the highest concentration of product can be formed before within a given timeframe, without degradation. Unfortunately, a large portion of biologically relevant molecules will denature or degrade at high enough temperatures, leading to efficiency losses.

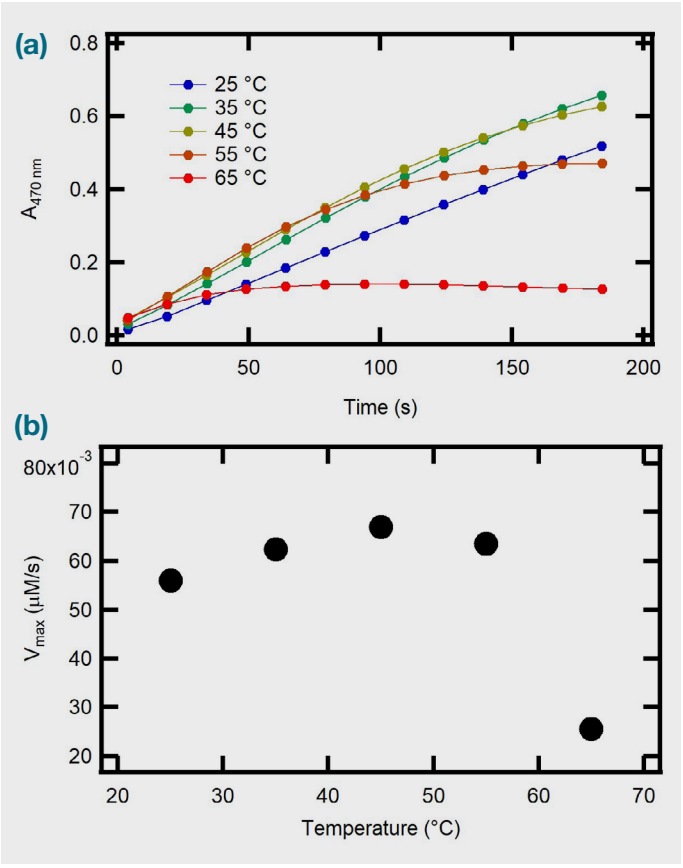

Figure 5: (a) Kinetic traces for the formation of tetraguaiacol at different reaction temperatures. Each sample includes 0.877 nM HRP, 15.8 mM guaiacol and 0.2 mM H_2O_2. (b) Calculated V_{max} as a function of reaction temperature.

To demonstrate this affect, the same HRP-catalyzed reaction was carried out at multiple different reaction temperatures. Figure 5a includes the kinetic traces for reaction solutions all containing 0.2 mM H_2O_2, held at varying temperatures. As is shown, increasing the temperature from 25 ˚C to 35 ˚C leads to a marked increase in the reaction rate, however an increase from 35 ˚C to 45 ˚C causes a slight rate improvement over the early time points, but begins to break from a linear curve at later reaction times. For traces collected at 55 ˚C and 65 ˚C, the reaction is effectively stopped, if not slowed, at earlier timepoints, leading to a lower overall tetraguaiacol concentration over the course of the reaction. Table 3 includes the calculated Michaelis-Menten parameters for each reaction temperature.

Reaction temperature (˚C)	V_{max} (µM/s)	K_m (mM)
25	0.21 ± 0.02	0.18 ± 0.05
35	0.31 ± 0.03	0.23 ± 0.03
45	0.38 ± 0.06	0.29 ± 0.09
55	0.39 ± 0.03	0.29 ± 0.05
65	0.4 ± 0.1	0.7 ± 0.4

Table 3: Calculated Michaelis-Menten parameters for reactions performed at different temperatures.

Figure 5b includes a plot of V_{max}, calculated through the Michaelis-Menten analysis, as a function of temperature. As can be shown, the maximum reaction rate stops increasing at temperatures higher than 45 ˚C, suggesting the enzyme is degrading at these higher temperatures. The plot in Figure 5b suggests the optimal temperature for this reaction is 45 ˚C, however the kinetic traces suggest the reactions performed at 35 ˚C are able to produce a slightly higher concentration of tetraguaiacol over the studied timeframe. For a more detailed analysis of the most favorable temperature, the experiment could be repeated with finer changes to the temperature than the 10 ˚C steps shown herein.

Evolution One UV-Visible Spectrophotometer.

Conclusion

Through the use of the Evolution One UV-Visible Spectrophotometer, the reaction kinetics at different temperatures were monitored for the HRP-catalyzed formation of tetraguaiacol. As is shown through the Michaelis-Menten analysis, the maximum reaction rate increases as temperature increases up to a reaction temperature of 45 ˚C. However, beyond 45 ˚C, the efficacy of HRP as a catalyst is diminished, likely as a result of denaturation, and the maximum reaction rate begins to lower. As shown through the above experiments, the ability to simultaneously perform temperature-controlled measurements using the 6-cell Rotary Peltier can be very helpful when characterizing enzymes. This is especially true for experiments which require multiple samples be monitored, like those needed for Michaelis-Menten analysis.

References

1. Hashim, F.J.; Vichitphan, S.; Han, J.; Vichitphan, K., Alternative Approach for Specific Tyrosinase Inhibitor Screening: Uncompetitive Inhibition of Tyrosinse by Moringa oleifera, Molecules, **2021**, 26, 4576.
2. Meghwanshi, G.K.; Kaur, N.; Verma, S.; Dabi, N.K.; Vashishtha, A.; Charan, P.D.; Purohit, P.; Bhandari, H.S.; Bhojak, N.; Kumar, R., Enzyme for Pharmaceutical and Therapeutic Applications, Biotechnol. Appl. Biochem., **2020**, 4, 586–601.
3. Berg, J.M.; Tymoczko, J.L.; Stryer, L., Enzymes: Basic Concepts and Kinetics. In Biochemistry, 5th ed.; W.H. Freeman and Company, **2002**, 189–225.
4. Thermo Fisher Scientific, Monitoring enzyme kinetics using UV-Visible absorption spectroscopy Michealis-Menten analysis, https://assets.thermofisher.com/TFS-Assets/MSD/Application-Notes/monitoring-enzyme-kinetics-uv-visible-absorption-spectroscopy-an56399.pdf
5. Peterson, M. E.; Daniel, R. M.; Danson, M. J.; Eisenthal, R., The Dependence of Enzyme Activity on Temperature: Determination and Validation Parameters, Biochem. J., **2007**, 402, 331–337.
6. Shannon, M. D.; Simmons, J., A Full-Semester Biochemistry Laboratory Synchronous with Lecture to Enhance Student Learning and Engagement, J. Chem. Ed., **2024**, 101, 1489–1498.
7. de Aspuru, E. O.; Zatón, A. M. L., Effect of Glutathione on Horseradish Peroxidase Activity, Spectrochim. Acta A Mol. Biomol. Spectrosc., **1999**, 55, 2343–2346.